Casati Paula (Orcid ID: 0000-0002-3194-4683)

AtCAF-1 mutants show different DNA damage responses after UV-B than those activated by other genotoxic agents in leaves

Evangelina Maulión[1,2], María Sol Gomez[1,2], Claudia Anabel Bustamante[1] and Paula Casati[1,*]

[1]Centro de Estudios Fotosintéticos y Bioquímicos (CEFOBI), Universidad Nacional de Rosario, Suipacha 531, 2000 Rosario, Argentina.

[2]These authors contributed equally to this article

[*]Correspondance: Paula Casati (casati@cefobi-conicet.gov.ar)

FUNDING: This research was supported by FONCyT grants PICT 2016-141 and 2015-157; and L`Oreal-UNESCO "For Women in Science" Award (Argentina).

Abstract

CAF-1 is a histone H3/H4 chaperone that participates in DNA and chromatin interaction processes. In this manuscript, we show that organs from CAF-1 deficient plants respond differently to UV-B radiation than to other genotoxic stresses. For example, CAF-1 deficient leaves tolerate better UV-B radiation, showing lower CPD accumulation, lower inhibition of cell proliferation, increased cell wall thickness, UV-B absorbing compounds and ploidy levels; while previous data from different groups have shown that CAF-1 mutants show shortening of telomeres, loss of 45S rDNA and increased homologous recombination, phenotypes associated to DNA breaks. Interestingly, CAF-1 deficient roots show increased inhibition of primary root elongation, with decreased meristem size due to a higher inhibition of cell proliferation after UV-B exposure. The decrease in root meristem size in CAF-1 mutants is a consequence of defects in programmed cell death after UV-B exposure. Together, we provide evidence demonstrating that root and shoot meristematic cells may have distinct protection mechanisms against CPD accumulation by UV-B, which may be linked with different functions of the CAF-1 complex in these different organs.

Keywords: cell proliferation, chromatin, DNA damage, histone chaperones, UV-B radiation.

We provide evidence that demonstrate that UV-B radiation that produce CPDs activate different DNA damage response mechanisms than other DNA damaging agents which require CAF-1 activity; and that root and shoot meristematic cells may have distinct protection mechanisms against DNA damage by UV-B.

1 INTRODUCTION

Plants are continually exposed to solar radiation because they are sessile organisms. Ultraviolet-B radiation (UV-B, 290-315 nm) is part of the solar spectrum; this radiation produces damage to different biomolecules, in particular to the DNA (Britt, 1996; Gerhard et al., 1999; Casati & Walbot, 2004). To avoid this damage, plants have mechanisms to filter or absorb UV-B to protect them (Emiliani et al., 2013 and 2018), and different DNA repair systems to remove or tolerate these lesions (Bray & West, 2005; Hays, 2002; Kimura & Sakaguchi, 2006).

The reduction in the leaf area is one of the plant responses after irradiation with UV-B (Wargent et al., 2009a and b; Fierro et al., 2015; Casadevall et al., 2013; Yan et al., 2012; Fina et al., 2017a). This reduction can be a consequence of a decrease in cell proliferation and/or in cell expansion, depending on the conditions of the treatment (Hectors et al., 2010). Previously, we demonstrated that in Arabidopsis and maize proliferating leaves exposed to UV-B, there is an inhibition of cell proliferation regulated by miR396, which inhibits the expression of *GROWTH REGULATING FACTORS* (*GRF*) transcription factors (Casadevall et al., 2013; Fina et al., 2017a). Moreover, we showed that another transcription factor, E2Fc, also participates in the regulation of cell proliferation under UV-B (Gomez et al., 2018). *E2Fc* deficient plants show a lower inhibition of leaf growth under UV-B conditions that damage DNA and decreased programmed cell death after exposure with altered *SOG1* and *ATR* expression. Interestingly, under UV-B conditions, E2Fc has an epistatic role over the miR396 pathway.

The decrease in leaf size can also be due to a reduction in the cell area, changes in cell area have been related to variations in cell ploidy because of endoreduplication. Changes in ploidy levels after UV-B exposure have been reported, and although the physiological role of this is not clear, an hypothesis is that endoreduplication would maintain a functional gene copy in case of damage (for a review, see Inzé & De Veylder, 2006).

Absorption of UV-B by DNA molecules produces the formation of cyclobutane pyrimidine dimers (CPD) and pyrimidine (6-4) pyrimidone photoproducts (6-4PPs) (Friedberg et al., 1995). This DNA damage disturbs base pairing and blocks DNA metabolism, including replication and transcription if damage continue, or results in mutations if photoproducts are bypassed by error-prone DNA polymerases (Britt, 1996). Besides UV-B, different endogenous and exogenous stresses can cause DNA damage, and plants have mechanisms to respond to these damages. DNA damage response in plants are regulated by the activity of two related kinases, ATAXIA TELANGIECTASIA MUTATED (ATM), which is mostly activated by double-strand breaks; and ATM AND RAD3 RELATED (ATR), mainly activated by single-strand breaks or stalled replication forks, for example CPDs and 6-4PPs (Culligan et al., 2006). However, in Arabidopsis, both ATR and/or ATM can activate DNA damage responses after UV-B exposure (Furukawa et al., 2010). Both ATM and ATR can activate different downstream regulators to activate responses like DNA repair, cell cycle arrest, endoreduplication or programmed cell death (Culligan et al., 2006).

The access of DNA to DNA repair enzymes is restricted by chromatin structure (Verbsky & Richards, 2001; Pfluger & Wagner, 2007; Eberharter & Becker, 2002; Vaillant & Paszkowski, 2007). In particular, proteins known as histone chaperones interact with their corresponding histones to enable the assembly and disassembly of nucleosomes (Park et al., 2008; Avvakumov et al., 2011). In relation to their activity, histone chaperones can as either H3–H4 or H2A–H2B types. In *Arabidopsis thaliana*, the H3–H4 chaperones are Histone Regulatory Homolog A (HIRA), Chromatin Assembly Factor-1 (CAF-1) and Anti-Silencing Function1 (ASF1); while the H2A–H2B chaperones are Facilitates Chromatin Transcription (FACT), Nucleosome Assembly Protein1 (NAP1) and NAP1-Related Proteins (NRPs) (Zhu et al., 2012).

Previously, we demonstrated that in *Arabidopsis thaliana,* there are two ASF1 proteins that are mainly expressed in proliferative tissues, and *ASF1A* and *ASF1B* are targets of regulation of E2F transcription factors, suggesting that both of them are regulated during cell cycle progression (Lario

et al., 2013). Interestingly, ASF1A and ASF1B were associated with the UV-B induced DNA damage response in *Arabidopsis thaliana*. On the other hand, in Arabidopsis, CAF-1 is composed by three different subunits FASCIATA1 (FAS1), FAS2 and MULTICOPY SUPPRESSOR OF IRA1 (MSI1). *fas1* or *fas2* mutants, which show loss of CAF-1 function, have different defects, like atypical shoot and short-root phenotypes that are related with meristem problems (Kaya et al., 2001; Leyser & Furner, 1992), mitosis inhibition and cell cycle arrest, an increase in endoreduplication and trichome branching in leaves (Exner et al., 2006; Ramirez-Parra & Gutierrez, 2007, Chen et al., 2008). CAF-1 mutants also show modified positioning of nucleosomes (Jiang & Berger, 2017; Muñoz-Viana et al., 2017; Otero et al., 2016). These mutants also have altered expression of certain genes, including transcripts for DNA repair activities and for enzymes in cell wall synthesis and degradation (Mozgova et al., 2015; Ono et al., 2006; Schönrock et al., 2006). CAF-1 deficient plants also show DNA damage related phenotypes, including shortening of telomeres, loss of 45S rDNA (Mozgova et al., 2010; Muchova et al., 2015), and increased homologous recombination (Endo et al., 2006; Gao et al., 2012; Kirik et al., 2006; Varas et al., 2015). Interestingly, all these phenotypes are related to DNA damage produced by strand breaks, which usually activate DNA damage responses by ATM (Culligan et al., 2006). However, the role of *A. thaliana* CAF-1 under UV-B conditions that induce the formation of pyrimidine dimers has not been investigated. In this work, we have addressed the potential role of FAS1 and FAS2 in post-UV-B responses in relation to their known function as subunits of a histone chaperone complex. Using *fas1* and *fas2* mutants, we analyzed DNA damage accumulation after UV-B exposure, demonstrating that both mutants show lower damage than WT leaves, in the dark and also under light conditions that allow photorepair, in contrast to the increased DNA strand break phenotype previously reported (Mozgova et al., 2010; Muchova et al., 2015; Endo et al., 2006; Gao et al., 2012; Kirik et al., 2006; Varas et al., 2015), which could be a consequence of a different activation of DNA damage responses by ATM and ATR. We also here show that CAF-1 regulates leaf development under UV-B conditions, as *fas1*

and *fas2* proliferating leaves show a lower inhibition of cell proliferation than WT leaves. Interestingly, leaf cells in the mutants show a lower area after UV-B exposure than leaf cells in mutant control plants, which could be a consequence of an increase in the cell wall thickness after UV-B exposure. Our results show that CAF-1 also participates in the DNA damage response in the roots after UV-B exposure. Curiously, *fas1* and *fas2* mutants show a lower number of cells that undergo programmed cell death after 1 day of exposure; however, after 4 days of recovery, while WT roots are recovered, CAF-1 mutants still show meristematic cells that are dead. As a consequence, *fas1* and *fas2* mutants show a significantly shorter primary roots after UV-B exposure than WT plants. Our data therefore demonstrate that CAF-1 complex has a different role during DNA damage response after UV-B radiation in the leaves and in the roots.

2 MATERIALS AND METHODS

2.1. Plant Material and Growth Conditions

fas1-4 (SAIL_662_D10) and *fas2-4* (SALK_033228) mutants were described previously (Exner *et al*., 2006) and were kindly provided by Dr. Lars Henning and Dr. Iva Mozgová (Swedish University of Agricultural Sciences and Linnean Center for Plant Biology, Sweden). *fas2-3* (SALK_118525) seeds were obtained from the Arabidopsis Biological Resource Center. *A. thaliana* ecotype Columbia (Col-0) was used for all experiments. Homozygous *fas2-3* mutants were selected by PCR analysis using primers that flank the T-DNA insertion, by analysis of mRNA expression levels, and by evaluating the leaf phenotypes, comparing to those of *fas2-4* mutants (Figure S1). Arabidopsis plants were sown on soil and kept in the dark at 4ºC. Plants were moved to a growth chamber after 3 days and they were grown at 22ºC under a 16h/8h light/dark photoperiod (100 $\mu Em^{-2}s^{-1}$). For most UV-B experiments, plants were irradiated with UV-B lamps for 4 h using fixtures mounted 30 cm

above the plants (2 W m^{-2} UV-B and 0.6 W m^{-2} UV-A, Bio-Rad ChemiDoc^{TM} XRS UV-B lamps, catalog 1708097). The lamps have emission spectra from 290-310 nm, and a peak at 302 nm. The bulbs were covered using cellulose acetate filters (CA, 100 mm extra-clear cellulose acetate plastic, Tap Plastics, Mountain View, CA); the CA filter absorbs wavelengths lower than 290 nm without removing UV-B from longer wavelengths. This control was done in case some lower wavelength radiation was produced with lamps aging. As a no UV-B control, plants were exposed for the same period of time under the same lamps covered additionally with a polyester plastic that absorbs UV-B at wavelengths lower than 320 nm (PE, 100 mm clear polyester plastic; Tap Plastics; 0.04 W m^{-2} UV-B and 0.5 W m^{-2} UV-A). UV radiation was recorded using a UV-B/UV-A radiometer (UV203 AB radiometer; Macam Photometrics). Leaves for qRT-PCR were collected immediately after treatment, while those used for cell expansion and cell wall thickness were collected one week after the end of the treatments. Leaves used to phenotypic analysis of ploidy levels and cell proliferation were collected at the end of leaf #5 expansion.

Seedlings for qRT-PCR were grown in Petri dishes. Sterilized seeds were grown on Murashige and Skoog (MS) growth medium without sugars, and were kept in a vertical position in the growth chamber. After five days of growth, seedlings were UV-B irradiated for 1 h (2 W m^{-2} UV-B) and collected immediately after the treatment. To collect the roots for qRT-PCR, we proceed in the same way, but when the treatments were finished, they were separated with a razor blade and frozen at -80ºC. For primary root elongation analysis, seedlings were grown and UV-B irradiated in the same way.

2.2. DNA Damage Analysis

CPD accumulation was analyzed by dot-blot analysis using monoclonal antibodies against CPDs (TDM-2) from Cosmo Bio Co., Ltd. (Japan). 2-week-old plants were irradiated with UV-B during

4h, and immediately after the treatment or 2h after the end of the UV-B treatment, both under light and under dark conditions, samples (0.1 g) were collected, immersed in liquid nitrogen and stored at -80ºC. 2 μg of the extracted DNA using a modified cetyl-trimetyl-ammonium bromide (CTAB) method was denatured in 0.3 M NaOH for 10 min. Samples were dot blotted onto a nylon membrane (Perkin Elmer life Sciences, Inc.) in sextuplicate. The blotted membrane was incubated for 2h at 80ºC and then blocked with a buffer containing 20 mM Tris-HCl, pH 7.6, 137 mM NaCl (TBS) and 5% (p/v) dried milk for 1 h at room temperature at 4ºC. Then, the membrane was washed with TBS and incubated with TDM-2 antibodies (1:2000 in TBS) overnight at 4ºC with agitation. Unbound antibody was washed away and secondary antibody conjugated to alkaline phosphatase (1:3000; BioRad) was added. The blot was washed several times and it was developed by the addition of 5-bromo-4-chloro-3-indolyl phosphate and nitroblue tetrazolium. Quantification was done by densitometry of the dot blots using ImageQuant software version 5.2. DNA was quantified fluormetrically using the Qubit dsDNA assay kit (Invitrogen), and checked in a 1% (w/v) agarose gels after quantification.

2.3. Quantitative RT-PCR

Total RNA was isolated from 20 mg of tissue using the TRIzol reagent (Invitrogen) as described in the manufacturer's protocol. Then, 0.5 to 1.0 mg of total RNA was incubated with RNase-free DNase I (1 unit/mL) following the protocol provided by the manufacturer to remove possible genomic DNA. The RNA was reverse-transcribed into first-strand cDNA using SuperScript II reverse transcriptase (Invitrogen); oligo(dT) and stem-loop oligo for miRNA396 were used as primers. The resultant cDNA was used as a template for quantitative PCR amplification in a StepOne™ System apparatus (ThermoFisher Scientific), using the intercalation dye SYBRGreen I (Invitrogen) as a fluorescent reporter and Platinum Taq polymerase (Invitrogen). Primers for each of

the genes under study were designed using PRIMER3 software (Rozen and Skaletsky, 2000) in order to amplify unique 50- to 250-bp products (Table S1). Amplification conditions were performed under the following conditions: 2 min of denaturation at 94°C; 40 cycles at 94°C for 15 s, 55°C or 58°C for 30 s, and 72°C for 45 s, followed by a 10-min extension at 72°C. Three biological replicates were performed for each sample. Melting curves for each PCR were determined by measuring the decrease of fluorescence with increasing temperature (from 65 to 98°C). PCR products were run on a 2% (w/v) agarose gel to confirm the size of the amplification products and to verify the presence of a unique PCR product. Transcript levels were normalized to those of the *A. thaliana* calcium dependent protein kinase3 (*CPK3*, Table S1) and to values in Col-0 plants grown under control conditions in the absence of UV-B. The expression of this gene has been previously demonstrated not to be UV-B regulated in Arabidopsis (Ulm et al., 2004).

2.4. Rosette and Leaf Area Quantification

Twenty seeds were sown per tray, in a disposition to avoid superposition during plant growth. 12 days after sowing (DAS), a group of plants were irradiated with a single UV-B treatment during 4 h at 2 W m^{-2} UV-B; while a different group was maintained as control and were not UV-B irradiated. After the different treatments, the plants were maintained in a growth chamber in the absence of UV-B. Photographs were taken every 2 days, and total leaf or rosette area of each plant was quantified using the ImageJ software.

2.5. Microscopic Observations

Leaves were fixed using a solution containing 50 % (v/v) ethanol; 5 % (v/v) acetic acid and 3,7 % (v/v) formaldehyde; and they were cleared using a solution containing 200 g chloral hydrate, 20 g

glycerol, and 50 ml dH_2O (Casadevall et al., 2013). Leaf images were acquired using differential interference contrast (DIC) microscopy; and areas were quantified using the ImageJ software. Palisade leaf cells were observed by DIC microscopy, the area of palisade cells was quantified, and the leaf blade area was divided by cell area to calculate the total number of palisade cells in the subepidermal layer. Eighty palisade cells were measured per leaf to determine the cell area. Experiments were done in duplicate with at least 10 leaves with similar results.

2.6. Flow Cytometric Analysis of Leaf #5

Ten leaves were cut with a razor blade in 1 ml of a buffer containing 45 mM $MgCl_2$, 30 mM sodium citrate, 20 mM 3-[N-morpholino]propane- sulfonic acid, pH 7.0, and 1% Triton X-100. The supernatant was filtered over a 30 µm mesh and 1 µl of 4',6-diamidino-2-phenylindole from a stock of 1 mg ml^{-1} was added, supplemented with RNase (Thermo-Fisher) at 50 mg ml^{-1} . Then, the extracted was sorted through the Cell Sorter BD FACSAria II flow cytometer. The endoreduplication index (EI) was calculated from the percentage values of each ploidy class with the formula: EI=[(0x%2C)+(1x%4C)+(2x%8C)+(3x%16C)+(4x%32C)]/100 (Barrow & Meister, 2003). This experiment was done in triplicate, each time using 10 plants corresponding to each treatment/genotype. In every experiment, for each treatment/genotype, at least 5,000 nuclei were analyzed.

2.7. Cell wall Analysis

For staining with Calcofluor white, leaves were decolorized in 95% ethanol for 24 h and then incubated in the dark for at least 10 min in 17.5 µg ml^{-1} Calcofluor in 0.1M Tris-HCl (pH 9.0). Leaves were 3 times washed with a buffer containing 10 mM PO_4^{3-}, 137 mM NaCl, and 2.7 mM

KCl (pH 7.4). Leaf images were acquired by CLSM (Nikon C1) with a 40X objective. The excitation wavelength for was 440 nm, and emission was collected at 500-520 nm. Thickness of twenty cell walls was measured per leaf using the ImageJ software. Experiments were done in duplicate with at least five leaves with similar results.

2.8. Extraction of total UV-B absorbing compounds

One-half gram of fresh leaf tissue was frozen in liquid nitrogen and ground to a powder with a mortar and pestle. The powder was extracted for 8 h with 3 mL of acidic methanol (1% HCl in methanol), followed by a second extraction with 6 mL of chloroform and 3 mL of distilled water. The extracts were vortexed and then centrifuged 2 min at 3000x*g*. UV-B absorbing compounds were quantified by absorbance at 330 nm, and anthocyanins at 540 nm.

2.9. Root Length Measurements

Seedlings were grown in Petri dishes as described above. Seedlings were then irradiated with UV-B for 1 h (2 W m^{-2} UV-B) or kept in the absence of UV-B. After the different treatments, the seedlings were maintained in a growth chamber in the absence of UV-B. Plates were photographed 1, 2, 3 and 4 days after the treatments, and the images were examined using the ImageJ program. Root lengths were measured by using a line traced along the root.

2.10. Analysis of programmed cell death

After growing plants for 5 days in vertically oriented MS-plates, seedlings were irradiated with UV-B light as described above. UV-B-irradiated and non-irradiated control seedlings were then

incubated for 24 h or 96h in the growth chamber, and then PCD was analyzed as described by Furukawa et al. (2010). Root tips were stained using a modified pseudo-Schiff propidium iodide staining protocol and visualized by confocal laser scanning microscopy (Nikon C1) under water with a 40X objective. The excitation wavelength for propidium iodide–stained samples was 488 nm, and emission was collected at 520 to 720 nm. Dead (intensely PI-staining) cells in the vicinity of the quiescent center were counted and scored as dead cells per root.

2.11. Statistical Analysis

Statistical analysis was done using ANOVA models (Tukey test) or alternatively Student's t test (Welch's T-tests), using untransformed data.

2.12. Accession Numbers

Sequence data from this article can be found in the Arabidopsis Genome Initiative under the following locus: At1g65470 (FAS1), At5g64630 (FAS2).

3 RESULTS

3.1. *fas1* and *fas2* leaves accumulate lower DNA damage after UV-B exposure

The role of CAF-1 in DNA damage and repair of photoproducts, such as cyclobutane pyrimidine dimers (CPDs) that are produced after UV-B exposure has not been investigated. Thus, we focused on the potential role of this complex in the damage and repair of UV-B induced DNA damage. We grew Arabidopsis WT, *fas1-4* and *fas2* (*fas2-3* and *fas2-4*) plants in the growth chamber in the

absence of UV-B for 14 days after sowing (DAS). Plants were then exposed to UV-B for 4 h at an intensity of 2 W m^{-2} in the presence of white light that allows direct photorepair by photolyases. As a control, a different group of plants was irradiated with the same lamps covered with a plastic filter that absorbs UV-B. Leaf samples from both groups of plants were collected immediately after the end of the UV-B treatment. DNA was extracted and CPD accumulation was compared in mutant leaves relative to that in WT leaves using monoclonal antibodies specifically raised against them. In the absence of UV-B, the steady state levels of CPDs in WT and mutants were similar and very low. However, after 4h of UV-B exposure, more unrepaired lesions accumulated in WT leaves than in the mutants (Figure 1a). This difference was also observed when plants were irradiated under dark conditions (Figure 1b). Similar results were obtained when these plants were allowed to recover for 2h in the absence of UV-B, both in the dark and under light conditions (Figure 1b). Although repair is evident in both WT and mutant leaves after 2 h of recovery, the CAF-1 mutants show less CPDs than WT plants under all conditions analyzed (Figure 1b; Figure S2). Together, this result demonstrates that the lower accumulation of CPDs in the DNA by UV-B in leaves that are deficient in the expression of *FAS1* and *FAS2*, which can be due to lower DNA damage, contrasts to what was previously reported under other genotoxic conditions that produce DNA strand breaks.

To discard the possibility that mutations on *FAS1* and *FAS2* may affect the expression of DNA-repair enzymes, *UVR2* (encoding a CPD photolyase) and *UVR7* (encoding ERCC1, a DNA excision repair protein of the nucleotide excision repair system) transcript levels were analyzed by RT-qPCR in WT and mutant leaves. Similar increases in transcripts levels were measured in all plants after a 4h UV-B treatment (Figure 1c, d). These results indicate that major CPD removal mechanisms are unaffected in mutant plants, and that decreased CPD accumulation in the mutant plants is not because CAF-1 regulate the expression of CPD repair enzymes.

3.2. *fas1* and *fas2* mutants overcome the inhibition in leaf cell proliferation and endoreduplication by UV-B, but show decreased cell area after exposure

To investigate the consequences of lower CPD accumulation in *fas1* and *fas2* leaves in cell proliferation after UV-B exposure, we analyzed palisade cell number in fully expanded leaf #5 from WT and mutant plants that were irradiated with a single UV-B light treatment during 4h 12 days after stratification. At this moment, leaf #5 is emerging and has proliferating cells (Casadevall et al., 2013). As controls, cell number was also analyzed in fully expanded leaf #5 from plants that were not irradiated. While leaf #5 area in CAF-1 mutants is smaller than that of WT plants under both treatments; after UV-B exposure, plants from all lines show leaves of decreased size (Figure 2a,b; Figure S3). Interestingly, despite that the decrease in leaf #5 area by UV-B was similar in WT and mutant plants, *fas1* and *fas2* mutants showed a lower decrease in cell proliferation than WT plants after UV-B exposure (Figure 2e; Figure S2). This lower inhibition of cell proliferation may be a consequence of the lower DNA damage accumulated in the mutants after exposure.

Leaves from *fas1* and *fas2* plants have fewer cells with bigger areas than WT leaves (Figure 2c-e, Figure S3; Hisanaga *et al.*, 2013). While cell area was not changed by UV-B in WT leaves under our experimental conditions as previously reported (Casadevall *et al.*, 2013), cell size was significantly decreased in CAF-1 mutants after the treatment (Figure 2c,d; Figure S3). *fas1* and *fas2* mutant leaves have been previously shown to have cells with increased ploidy levels, which correlated with the increased cell area reported (Exner *et al.*, 2006). Differences in the cell size can be in part a consequence of the DNA content (Melaragno *et al.*, 1993; Sugimoto-Shirasu & Roberts, 2003). Therefore, to investigate if differences in cell area in leaf #5 of CAF-1 mutants after irradiation were due to changes in DNA ploidy, leaf #5 ploidy levels were measured through flow cytometry from UV-B irradiated plants, or from non-irradiated plants. Figure 2 (f,g) shows that, in CAF-1 mutants, ploidy levels were higher than those in Col-0 leaf #5, with a strong increase in the

relative amount of cells with 32C DNA content, as previously reported (Hisanaga *et al.*, 2013). In CAF-1 deficient leaves under control conditions, the endoreduplication index (EI) was higher than that of Col-0 plants (Figure 2f). These differences in EI correlate with measurements of cell area presented in Figure 2d. However, after UV-B exposure, while the EI of WT leaf #5 cells was not significantly changed, the calculated EI for *fas2* mutants showed a low but significant increase (Figure 2f). Therefore, the decrease in cell leaf area in CAF-1 mutants by UV-B is not a consequence of changes in ploidy levels. Conversely, the increase in EI after UV-B exposure measured in the mutants could instead be related to the lower DNA damage observed (Figure 1). Plants accumulating lower DNA damage may be able to faster resume endoreduplication in order to tolerate UV-B damaging conditions better.

3.3. *fas1* and *fas2* leaves show thicker cell walls after UV-B exposure and altered cell wall metabolism transcripts

Previously, Schönrock et al. (2006) analyzed the transcriptome of *fas1* and *fas2* mutants and showed that several transcripts encoding enzymes participating in cell wall metabolism were altered in the mutants. Therefore, we investigated weather changes in cell wall could be related with the decreased cell size measured in *fas1* and *fas2* leaf #5 after UV-B irradiation. As shown in Figure 3a and Figure S4, while cell wall thickness was similar in WT palisade leaf #5 cells from control and UV-B irradiated plants and CAF-1 mutant leaves from control plants; cell walls from *fas1* and *fas2* leaf #5 were significantly thicker in UV-B irradiated plants. This increase was correlated with changes in the expression of genes encoding cell wall metabolism enzymes in the mutant leaf #5 under control conditions and/or after UV-B exposure, which were previously shown to be differentially expressed in *fas1* and *fas2* mutants compared to WT plants (Schönrock et al., 2006; Figure 3c-g). As shown in Figure 3b, *XTH23,* encoding a cell wall modifying XYLOGLUCAN

ENDOTRANSGLUCOSYLASE/HYDROLASE 23, had increased expression levels in *fas1* and *fas2* mutants under control conditions, and a significant decrease after UV-B exposure, while transcripts levels in WT plants were low and were not changed after irradiation. In addition, *XTH9* and *XTH22* were different in WT compared to CAF-1 mutants (Figure 3c-d). Increased *XTH9* expression was reported to improve cell-wall loosening to allow rearrangement of the cell wall and subsequent cell expansion (Pholo et al., 2018). XTH enzymes have the potential to control plant cell growth; thus, changes in cell size measured after UV-B exposure in *fas1* and *fas2* mutants could be due to differences in XTH levels and activities.

Similarly, changes in the expression of the expansin *EXP1* have been related to loosening of the cell wall (Zhang et al., 2011); this gene was shown to be down-regulated by UV-B in Arabidopsis (Hectors et al., 2007). In our experiments, *EXP1* levels were significantly lower in CAF-1 mutants than in WT plants (Figure 3e). Moreover, transcripts for *PCL*, encoding a pectate lyase, were higher in the mutants than in WT plants (Figure 3f). Together, our results show that *fas1* and *fas2* mutants show altered expression of transcripts encoding enzymes participating in cell wall metabolism in leaves, and this could be at least one reason for the changes in cell wall and cell size measured after UV-B exposure in the mutants. Despite the fact that transcripts encoding some cell wall enzymes are also decreased after UV-B in WT plants, changes in expression levels of some transcripts after UV-B exposure, such as *XTH23* and *XTH9* (Figure S4b-f), are more important in CAF-1 deficient plants. Although the relative importance for UV-B tolerance of different enzymes may not be directly inferred from changes in gene expression, it is possible that these differences could account for the modifications in cell size and cell wall measured in the mutants after UV-B exposure.

3.4. CAF-1 mutants have higher accumulation of UV-B absorbing pigments

The lower CPD accumulation after UV-B exposure in CAF-1 mutants could be in part due to UV-B absorption by thicker cell walls. Besides cell walls, plants also synthesize other UV-B absorbing compounds, for example flavonoids, that can protect them against UV-B exposure. Therefore, we analyzed UV-B absorbing compound levels in WT and CAF-1 mutants under control conditions and after UV-B exposure. As shown in Figure 4, UV-B absorbing pigments and anthocyanins levels were higher in *fas1* and *fas2* mutants; both under control and UV-B conditions. Thus, higher levels of UV-B absorbing pigments in the mutants may protect the plants against CPD accumulation after UV-B exposure.

3.5. *fas1* and *fas2* mutants show increased inhibition of primary root elongation, decreased meristem size and defects in programmed cell death in the root meristem after UV-B exposure

Besides inhibiting leaf growth, UV-B inhibits primary root elongation (Dotto & Casati, 2017). Therefore, we also investigated if the CAF-1 complex has a role in primary root growth in seedlings exposed to UV-B. Figure 5 (a,b), and Figure S5 show that *fas1* and *fas2* mutants have a shorter primary root under control conditions than WT seedlings. Interestingly, primary root elongation was significantly more inhibited by UV-B in *fas1* and *fas2* than in WT plants (Figure 5c and Figure S5). Previously, Johnson et al. (2018) showed that in roots, the programmed destruction of the mitotically compromised stem cell niche after DNA damage triggers its regeneration, enabling growth recovery. Thus, to analyze if the higher decrease in root elongation could be due to defects in the induction of programmed cell death (PCD) in response to UV-B in the root meristem, we evaluated cell death in root tips (Furukawa et al., 2010; González Besteiro & Ulm, 2013; Falcone Ferreyra et al., 2016). While WT roots did not show any dead cells when they were kept under control conditions in the absence of UV-B, *fas1* and *fas2* mutants showed some dead cells, in agreement to data previously reported (Ma et al., 2018; Figure 5d-g). However, 1d after UV-B exposure, while both WT and *fas1*

and *fas2* roots accumulated dead cells, root tips from CAF-1 mutants showed significantly fewer dead cells compared to WT roots (Figure 5d,f, Figure S5e), suggesting that CAF-1 has a role in PCD after UV-B. Interestingly, 4d after the treatment, while UV-B irradiated WT roots recovered and dead cells were almost undetectable; the number of dead cells in irradiated *fas1* and *fas2* mutants was higher than in WT roots (Figure 5g and Figure S5f-g). Therefore, altered PCD in the primary roots of CAF-1 mutants after UV-B could be related to the decrease in root elongation rate after UV-B exposure.

Consequently, we analyzed weather altered PCD responses in the meristematic zone of CAF-1 mutant roots could affect meristem development. We therefore measured the meristem size, the number of cortex cells in the meristem and the length of the meristematic cortex cells after exposure. Four days after the treatment, *fas1* and *fas2* mutants have a shorter meristematic root zone than that of WT seedlings, and this was true both under control and in UV-B irradiated conditions (Figure 6a and Figure S6a). However, the decrease in the meristem length by UV-B was higher in the mutants than in WT primary roots (Figure 6b and Figure S6b). Interestingly, and in contrast to what we measured in irradiated proliferating leaves, the higher decrease in the meristem size of *fas1* and *fas2* roots was a consequence of a higher inhibition of cortex cell proliferation than that measured in WT roots (Figure 6c,d and Figure S6c,d); while the increase in cortex cell length determined in the meristems of all plants by UV-B was similar (Figure 6e,f and Figure S6e,f). Thus, UV-B affects leaf and root development in opposite ways in plants deficient in CAF-1. In the roots, altered PCD after exposure may affect meristem development, which in turn modifies growth of the elongating root.

3.6. CAF-1 mutants show altered expression of DNA damage response transcripts in different organs and after UV-B exposure

Finally, to analyze whether differences in UV-B responses could be a consequence of altered expression of DNA damage response transcripts in the different organs, we measured *ATM*, *ATR* and *SOG1* transcript levels in 6-d-old Arabidopsis WT and CAF-1 mutant seedlings that were grown under control conditions and immediately after a 4-h-UV-B treatment. Transcript levels were also analyzed in 6-d-old roots under the same treatments. As shown in Figure 7a, while *ATM* levels are increased after UV-B exposure in WT seedlings, up-regulation is not observed in CAF-1 seedlings. However, *ATM* is down-regulated by UV-B in roots from all seedlings. Similarly, *SOG1* is only also up-regulated by UV-B in WT seedlings, while UV-B exposure decrease transcript levels in roots from all lines (Figure 7c). Interestingly, under control conditions in the absence of UV-B, *ATM* and *SOG1* levels are higher in CAF-1 mutants than in WT plants, both in seedlings and in roots. In contrast, *ATR* is increased by UV-B in WT and mutant seedlings, with higher levels in *fas2* seedlings after UV-B exposure, while expression levels are similar in roots from all lines under all conditions (Figure 7b). Together, it is possible that the differences in UV-B responses in different organs observed in this work may be due to differences in expression patterns of DNA damage response transcripts in CAF-1 mutants.

4 DISCUSSION

In Arabidopsis, loss of CAF-1 function causes different defects, including shortening of telomeres, loss of 45S rDNA and an increase of both mitotic and meiotic homologous recombination frequencies (Endo et al., 2006; Gao et al., 2012; Kirik et al., 2006; Varas et al., 2015; Mozgova et al., 2010; Muchova et al., 2015). However, the effects of DNA damaging agents that produce stalled replication forks such us CPDs were not previously investigated in plants lacking CAF-1. While yeast CAF-1 mutants are viable but show enhanced sensitivity to UV light (Kaufman et al., 1997); our data demonstrate that Arabidopsis CAF-1 deficient plants show different sensitivity to UV-B in

the leaves and in the roots. In the leaves, *fas1* and *fas2* mutants show lower levels of CPDs after UV-B exposure than WT plants, both under light conditions and also in the absence of photorepair. This result seems to contradict previous data; however, all earlier studies were done analyzing DNA damage and repair processes that produce DNA strand breaks (Endo et al., 2006; Gao et al., 2012; Kirik et al., 2006; Varas et al., 2015; Mozgova et al., 2010; Muchova et al., 2015), while UV-B mostly induces the formation of crosslinks such as the CPDs and 6-4 photoproducts (Friedberg et al., 1995). As described in the Introduction, different types of DNA damage trigger the DNA damage response through the activation of two different kinases, ATM and ATR. While ATM is mostly activated by double-strand breaks, ATR is mostly activated by single-strand breaks or stalled replication forks (Harper & Elledge, 2007). However, in Arabidopsis, UV-B radiation may activate both kinases (Furukawa et al., 2010). Previously, Hisanaga et al. (2013) showed that activation of the DNA damage response and the lower number of cells in *fas1* leaves depend on the presence of ATM but not on ATR. Moreover, the high ploidy phenotype of *fas1* mutants is also suppressed in *ATM* deficient plants but not in *atr* mutants, suggesting that ATM but not ATR activation of the DNA damage response acts as an upstream trigger to regulate cell cycle progression and entry into the endocycle. Interestingly, in our experiments, while *ATM* and *SOG1* transcript levels are significantly increased after UV-B exposure in WT seedlings, up-regulation of these transcripts is not observed in CAF-1 mutants. However, transcript levels are significantly higher under control conditions. On the other hand, *ATR* levels are significantly higher in *fas2* seedlings after UV-B. Therefore, the UV-B responses observed in CAF-1 mutant leaves, which seem to be contrary to those reported previously under DNA damage conditions that produce double strand breaks, may be due to different activation and regulation of the DNA damage response by different DNA damaging agents. Although activation of the DNA damage response pathway is mainly by activation through protein phosphorylation, our results suggest that this activation may also occur through changes in *ATM, ATR* and *SOG1* levels.

On the other hand, CAF-1 mutants show altered chromatin structure; for example, CAF-1 deficient nuclei have reduced cytological heterochromatin content and nucleosome landscape changes (Schönrock et al., 2006; Stroud et al., 2013; Muñoz-Viana et al., 2017). While nearly 15% of the *Arabidopsis* genome is heterochromatic in WT plants, this fraction is reduced by 20–30% in CAF-1 deficient plants (Schönrock et al., 2006). Additionally, while globally most nucleosomes are not affected in CAF-1 mutants; certain non-transcribed regions, in particular in proximal promoters, show nucleosome depletion (Muñoz-Viana et al., 2017). Therefore, altered chromatin structure in CAF-1 deficient plants with reduced nucleosome occupancy or with nucleosome gaps may lead to a more widespread loosening of chromatin packing, allowing better repair of CPDs that are produced after UV-B exposure in the leaves, both by photolyases and by other repair systems. Alternatively or in addition, increased repair of CPDs may be a consequence of higher transcription of DNA repair genes. Higher expression levels of DNA repair genes, such as some related to homologous recombination and alternative non-homologous end-joining, were shown to be up-regulated in *fas1* and *fas2* plants (Schönrock et al., 2006; Varas et al., 2015). Despite this, *UVR2* and *UVR7* were similarly expressed and induced after UV-B exposure in leaves of CAF-1 mutants and WT plants in our experiments, suggesting that decreased CPD levels may not be due to increased expression of DNA repair enzymes.

Leaf cell walls in *fas1* and *fas2* mutants increase their thickness after UV-B exposure, these changes in cell wall properties may also raise their UV-B absorption properties, and as a consequence absorbance by cell wall components may protect the cells against DNA damage. Some plant cell wall components, such as phenolic compounds, have been previously demonstrated to act as UV-screening molecules, increasing tolerance against UV-B (Machinandiarena et al., 2018; Ruiz et al., 2016; Pontin et al., 2010). Moreover, our results show that CAF-1 mutants accumulate higher levels of soluble UV-B absorbing compounds, similarly as what is was previously shown in *det1* mutants, which have altered chromatin architecture and accumulate higher UV sunscreen

compounds (Castells et al., 2010). Thus, altered expression of DNA damage response transcripts, changes in chromatin structure that facilitates the repair of CPDs, increased absorption of UV-B by cell wall components and other UV-B absorbing molecules, and/or changes in expression levels of DNA repair enzymes different to photolyases (for example participating in repair by recombination) may be the cause(s) of the lower CPD levels in CAF-1 mutants after UV-B exposure in Arabidopsis leaves.

We here also demonstrate that lower CPD accumulation after UV-B exposure in the leaves of CAF-1 mutants is accompanied by a lower inhibition of cell proliferation. Cell division is a primordial process in plant life and is tightly regulated to allow plant growth and development. When DNA is damaged, cell cycle progression is impaired; therefore, lower DNA damage may allow *fas1* and *fas2* plants to resume cell division faster than WT plants. Despite this, we cannot rule out that the extent of developmental severity of the untreated CAF-1 mutant phenotype may not allow for identification of UV-B-aggravated effects that could be additive to the already existing defects. Lower CPDs accumulation in CAF-1 mutants may therefore result in a faster resumption of DNA replication. Interestingly, CAF-1 mutants also show increased ploidy levels in UV-B irradiated leaf #5, which was proliferating at the moment of the treatment; however, this increase in ploidy levels was not observed in WT leaf #5. It was previously suggested that plants with improved DNA repair abilities, such as plants deficient in the expression of the E2Fe transcription factor, which is a negative regulator of the expression of the *UVR2* photolyase in Arabidopsis, resume endoreduplication faster than control plants, contributing in this manner to UV-B radiation resistance (Radziejwoski et al., 2011). Endoreduplication has been suggested to participate in the protection against UV-B radiation, for example the *uvi4* mutant displays increased DNA ploidy levels and increased UV-B tolerance (Hase et al., 2006). One hypothesis is that the presence of multiple copies of important genes by endoreduplication could reduce the risk of losing essential genes when mutated; or they could help repair damaged copies by homologous recombination using

an intact copy as a template (Kondorosi & Kondorosi, 2004). Alternatively, endoreduplication may sustain tissues growth by supporting cell expansion under conditions that inhibit cell proliferation (Barow & Meister, 2003). In our experiments, increased endoreduplication in leaf cells is not accompanied with an increase in cell size; on the contrary, while CAF-1 mutants have larger cells than those in WT leaves under control conditions, UV-B exposure stimulates a decrease in cell size in *fas1* and *fas2* mutants that is not observed in WT cells. Exner et al. (2006) have also previously shown that in CAF-1 mutant leaves, epidermal cells were significantly larger than those in the WT plants, with reduced number of cells. Interestingly, they also showed that CAF-1 is required to restrict branching of leaf trichomes. However, increased trichome branching in *fas2* mutants was not strictly correlated with increased nuclear DNA content that is usually associated with trichome development. Moreover, although cell elongation was impaired in *fas2* hypocotyls, seedlings showed increased DNA endoreduplication (Exner et al., 2006). We here show that the decrease in cell area in CAF-1 mutants by UV-B can be a consequence of an increase in cell wall thickness. This increase in cell wall width could be related to changes in the expression levels of enzymes that metabolize plant cell walls in CAF-1 mutants (Figure 3, Schönrock et al., 2006). Interestingly, Arabidopsis plants with different somatic ploidy levels have altered cell wall composition. Cell wall characterization of these plants showed that the basic somatic ploidy level negatively correlated with lignin and cellulose, and positively correlated with hemicellulose and pectin content in the stems (Corneillie et al., 2019). Therefore, under UV-B conditions, the increase in cell wall thickness in proliferating leaves from CAF-1 mutants could be a consequence of increased ploidy levels.

We here show that roots of CAF-1 seedlings are shorter than those of WT seedlings, in agreement to previous data (Ma et al., 2018). CAF-1, together with the H2A/H2B histone chaperone NAP1-RELATED PROTEIN1/2 (NRP1/2), participates in the maintenance of the root stem-cell niche in Arabidopsis; *fas2-4* mutants have reduced primary root growth, showing a decrease in the length of the root meristematic zone with reduced number of cells (Ma et al., 2018). Our results

demonstrate that CAF-1 mutants also show a higher inhibition of primary root elongation after UV-B exposure than roots from WT seedlings, and this is because the meristematic zone of *fas1* and *fas2* plants is significantly shorter than that from WT roots after exposure. The root meristem of CAF-1 deficient seedlings shows a significant higher decrease in cortex cell number than WT roots after UV-B exposure. Interestingly, cortex cells in the root meristem are larger after irradiation in all genotypes. These results are very surprising, as they are opposite to those determined in the leaves, where cell proliferation is less inhibited and cell size is decreased in CAF-1 mutants after UV-B exposure. Previous results have shown that transcript levels of several key regulatory genes involved in root growth and patterning are modified in *fas2-4* roots, altered expression of these transcripts are associated with chromatin changes in the mutant (Ma et al., 2018). Specific expression changes in genes that regulate root growth may account for the phenotypic differences observed after UV-B exposure on leaves and roots in this work. Interestingly, Ma et al. (2018) demonstrated that under control conditions, *fas2-4* roots showed programmed cell death and high levels of the DNA damage mark histone H2A.X phosphorylation, suggesting that CAF-1 mutants are under constant genotoxic stress. This is in agreement with the results presented here. However, one day after UV-B exposure, *fas1* and *fas2* roots show less dead cells than WT roots, but 4 days after the end of the treatment, while WT roots are recovered and only show a few dead cells, *fas1* and *fas2* have more dead cells than WT roots, both in control plants and after exposure. In this way, the higher number of meristematic root dead cells can probably be related with the decreased size in the meristematic zone of CAF-1 mutants measured. Our data show that, in the roots, *ATM* and *SOG1* levels are higher in CAF-1 mutants under controls conditions; therefore, defects in PCD in the mutant roots may be a consequence of altered activation of the DNA damage response. Interestingly, *sog1* mutants are defective in damage-induced programmed cell death, they maintain the cell identities and structure of the stem cell niche immediately after exposure to a genotoxic stress, but meristematic cells fail to undergo cell division after longer exposure times, stopping root growth (Johnson et al., 2018). SOG1

requires to be phosphorylated by ATM or other kinases to activate DNA damage responses (Yoshiyama et al., 2013); therefore, in Arabidopsis roots, but not in leaves, a mutation in *fas1* or *fas2* genes could impair ATM phosphorylation of SOG1 during UV-B exposure, which in turn may alter activation of the DNA damage response and PCD in particular. This data suggests that CAF-1, together with NRP1/2, maintain genome integrity that is important for appropriate stem-cell niche function during root development.

In conclusion, we here show that organs from CAF-1 deficient plants show different (and sometimes opposite) phenotypes when exposed to UV-B radiation. While the leaves seem to tolerate better UV-B radiation, with decreased DNA damage, cell proliferation and cell area; and increased cell wall thickness, accumulation of UV-B absorbing compounds and ploidy levels; the roots show increased inhibition of primary root elongation, with decreased meristem size due to a higher inhibition of cortex cell proliferation and increased cortex cell length. Previously, differences in root and shoot development in *fas2* mutants were also reported (Ma et al., 2018). Therefore, the root and shoot meristematic cells may have distinct protection mechanisms against DNA damage and activation of the DNA damage response by UV-B, which may be linked with different functions of the CAF-1 complex in these different organs.

AUTHOR CONTRIBUTIONS

E.M., M.S.G. and P.C. conceived and designed the study. E.M., M.S.G., C.A.B. and P.C. performed the experiments. E.M., M.S.G. and P.C. analyzed data. P.C. wrote the paper.

ACKNOWLEDGMENTS

This research was supported by FONCyT grants PICT 2016-141 and 2015-157; and L`Oreal-UNESCO “For Women in Science” Award (Argentina) to P.C. P.C. and C.B. are members of the

Researcher Career of CONICET and Professors at UNR. E.M was a postdoctoral fellow from CONICET and M.S.G is a doctoral fellow from the same Institution. We thank Dr. Lars Henning and Dr. Iva Mozgová for *fas1* and *fas2* seeds, María José Maymó for care in cultivating Arabidopsis plants.

REFERENCES

Avvakumov, N.A., Nourani. J., & Cote. J. (2011). Histone chaperones: modulators of chromatin marks. *Molecular Cell*, 41, 502–514.

Barow, M., & Meister, A. (2003). Endopolyploidy in seed plants is differently correlated to systematics, organ, life strategy and genome size. *Plant Cell and Environment*, 26, 571–584.

Bray, C.M., & West, C.E. (2005). DNA repair mechanisms in plants: crucial sensors and effectors for the maintenance of genome integrity. *New Phytologist*, 168, 511–528.

Britt, A.B. (1996). DNA damage and repair in plants. *Annual Review of Plant Physiology and Plant Molecular Biology*, 47, 75-100.

Casadevall, R., Rodriguez, R.E., Debernardi, J.M., Palatnik, J.F., & Casati, P. (2013). Repression of growth regulating factors by the microRNA396 inhibits cell proliferation by UV-B radiation in Arabidopsis leaves. *The Plant Cell*, 25, 3570–3583.

Casati, P., & Walbot, V. (2004). Crosslinking of ribosomal proteins to RNA in maize ribosomes by UV-B and its effects on translation. *Plant Physiology*, 136, 3319-3332.

Castells, E., Molinier, J., Drevensek, S., Genschik, P., Barneche, F., & Bowler, C. (2010) *det1-1*-induced UV-C hyposensitivity through *UVR3* and *PHR1*photolyase gene over- expression. *Plant Journal*, 63, 392-404.

Chen, Z., Tan, J.L., Ingouff, M., Sundaresan, V., & Berger, F. (2008). Chromatin assembly factor 1 regulates the cell cycle but not cell fate during male gametogenesis in Arabidopsis thaliana. *Development,* 135, 65-73.

Corneillie, S., De Storme, N., Van Acker, R., Fangel, J.U., De Bruyne, M., De Rycke, R., Geelen, D., Willats, W.G.T., Vanholme, B., & Boerjan, W. (2019). Polyploidy affects plant growth and alters cell wall composition. *Plant Physiology,* 179, 74-87.

Culligan, K.M., Robertson, C.E., Foreman, J., Doerner, P., & Britt, A.B. (2006). ATR and ATM play both distinct and additive roles in response to ionizing radiation. *Plant Journal*, 48, 947–961.

Dotto, M., & Casati, P. (2017). Developmental reprogramming by UV-B radiation in plants. *Plant Science*, 267, 96-101.

Eberharter, A., & Becker, P.B. (2002). Histone acetylation: A switch between repressive and permissive chromatin. Second in review on chromatin dynamics. *EMBO Reports,* 3, 224-229.

Emiliani, J., D'Andrea, L., Falcone Ferreyra, M.L., Maulión, E., Rodriguez, E., Rodriguez-Concepción, M., & Casati, P. (2018). A role for β,β-xanthophylls in Arabidopsis UV-B photoprotection. *Journal of Experimental Botany,* 69, 4921-4933.

Emiliani, J., Grotewold, E., Falcone Ferreyra, M.L., & Casati, P. (2013). Flavonols Protect Arabidopsis Plants against UV-B Deleterious Effects. *Molecular Plant,* 6, 1376-1379.

Endo, M., Ishikawa, Y., Osakabe, K., Nakayama, S., Kaya, H., Araki, T., Shibahara, K., Abe, K., Ichikawa, H., Valentine, L., Hohn, B., & Toki, S. (2006). Increased frequency of homologous recombination and T-DNA integration in Arabidopsis CAF-1 mutants. *The EMBO Journal*, 25, 5579-5590.

Exner, V., Taranto, P., Schonrock, N., Gruissem, W., & Hennig, L. (2006). Chromatin assembly factor CAF-1 is required for cellular differentiation during plant development. *Development,* 133, 4163-4172.

Falcone Ferreyra, M.L., Casadevall, R., D'Andrea, L., AbdElgawad, H., Beemster, G.T., & Casati, P. (2016). AtPDCD5 plays a role in programmed cell death after UV-B exposure in Arabidopsis. *Plant Physiology,*170, 2444-2460.

Fierro, A.C., Leroux, O., De Coninck, B., Cammue, B.P.A., Marchal, K., Prinsen, E., Van Der Straeten, D., & Vandenbussche, F. (2015). Ultraviolet-B radiation stimulates downward leaf curling in *Arabidopsis thaliana*. *Plant Physiology and Biochemistry,* 93, 9–17.

Fina, J.P., Casadevall, R., AbdElgawad, H., Prinsen, E., Markakis, M., Beemster, G.T., & Casati, P. (2017a). UV-B inhibits leaf growth through changes in Growth Regulating Factors and gibberellin levels. *Plant Physiology,* 174, 1110-1126.

Fina, J.P., Masotti, F., Rius, S.P., Crevacuore F, & Casati P. (2017b). HAC1 and HAF1 Histone Acetyltransferases have different roles in UV-B Responses in Arabidopsis. *Frontiers in Plant Science,* 8, 1179.

Friedberg, E.C., Walker, G.C., & Siede, W. (1995). DNA damage. Washington, DC: *ASM Press.*

Furukawa, T., Curtis, M.J., Tominey, C.M., Duong, Y.H., Wilcox, B.W.L., Aggoune, D., Hays, J.B., & Britt, A.B. (2010). A shared DNA-damage-response pathway for induction of stem-cell death by UVB and by gamma irradiation. *DNA Repair (Amst.),* 9, 940–948.

Galbraith, D.W., Harkins, K.R., Knapp, S. (1991). Systemic endopolyploidy in *Arabidopsis thaliana*. *Plant Physiology,* 96, 985-989.

Gao, J., Zhu. Y., Zhou. W., Molinier, J., Dong, A., Shen, & W.H. (2012). NAP1 family histone chaperones are required for somatic homologous recombination in Arabidopsis. *The Plant Cell,* 24, 1437-1447.

Gómez, M.S., Falcone Ferreyra, M.L., Sheridan, M.L., & Casati, P. (2018). Arabidopsis E2Fc is required for the DNA damage response under UV-B radiation epistatically over the microRNA396 and independently of E2Fe. *Plant Journal,* https://doi.org/10.1111/tpj.14158

González Besteiro, M.A., & Ulm, R. (2013). ATR and MKP1 play distinct roles in response to UV-B stress in Arabidopsis. *Plant Journal*, 73, 1034-1043.

Harper, J.W., & Elledge, S.J. (2007). The DNA damage response: ten years after. *Molecular Cell*, 28, 739–745.

Hase, Y., Trung, K.H., Matsunaga, T., & Tanaka, A. (2006). A mutation in the uvi4 gene promotes progression of endo-reduplication and confers increased tolerance towards ultraviolet B light. *Plant Journal*, 46, 317–326.

Hays, J.B. (2002). Arabidopsis thaliana, a versatile model system for study of eukaryotic genome-maintenance functions. *DNA Repair*, 1, 579-600.

Hectors, K., Jacques, E., Prinsen, E., Guisez, Y., Verbelen, J.P., Jansen, M.A.K., Vissenberg, K. (2010). UV radiation reduces epidermal cell expansion in leaves of Arabidopsis thaliana. *Journal of Experimental Botany*, 61, 4339–4349.

Hectors, K., Prinsen, E., De Coen, W., Jansen, M.A.K., & Guisez, Y. (2007). Arabidopsis thaliana plants acclimated to low dose rates of ultraviolet B radiation show specific changes in morphology and gene expression in the absence of stress symptoms. *New Phytologist*, 175, 255–270.

Hisanaga, T., Ferjani, A., Horiguchi, G., Ishikawa, N., Fujikura, U., Kubo, M., Demura, T., Fukuda, H., Ishida, T., Sugimoto, K., & Tsukaya, H. (2013). The ATM-Dependent DNA Damage Response Acts as an Upstream Trigger for Compensation in the fas1 Mutation during Arabidopsis Leaf Development. *Plant Physiology*, 162, 831–841.

Inzé, D., & De Veylder, L. (2006). Cell cycle regulation in plant development. *Annual Reviews in Genetics*, 40, 77–105.

Jiang, D., & Berger, F. (2017). DNA replication-coupled histone modification maintains Polycomb gene silencing in plants. *Science*, 357, 1146-1149.

Johnson, R.A., Conklin, P.A., Tjahjadi, M., Missirian, V., Toal, T., Brady, S.M., & Britt, A.B. (2018). SUPPRESSOR OF GAMMA RESPONSE1 Links DNA Damage Response to Organ Regeneration. *Plant Physiology,* 176, 1665–1675.

Kaufman, P.D., Kobayashi, R., & Stillman, B. (1997). Ultraviolet radiation sensitivity and reduction of telomeric silencing in *Saccharomyces cerevisiae* cells lacking Chromatin Assembly Factor-1. *Genes and Development,* 11, 345–357.

Kaya, H., Shibahara, K.I, Taoka, K.I., Iwabuchi, M., Stillman, B., & Araki, T. (2001). FASCIATA genes for chromatin assembly factor-1 in arabidopsis maintain the cellular organization of apical meristems. *Cell*, 104, 131-142.

Kimura, S., & Sakaguchi, K. (2006). DNA Repair in Plants. *Chemical Reviews,* 106, 753-766.

Kirik, A., Pecinka, A., Wendeler, E., & Reiss, B. (2006). The chromatin assembly factor subunit FASCIATA1 is involved in homologous recombination in plants. *The Plant Cell,* 18, 2431-2442.

Kondorosi, E., & Kondorosi, A. (2004). Endoreduplication and activation of the anaphase-promoting complex during symbiotic cell development. *FEBS Letters,* 567, 152–157.

Lario, L., Ramirez-Parra, E., Gutierrez, C., Spampinato, C., & Casati, P. (2013). ASF1 Proteins are involved in UV-induced DNA damage repair and are cell cycle regulated by E2F transcription factors in *Arabidopsis thaliana*. *Plant Physiology*, 162, 1164-1177.

Leyser, H.M., & Furner, L.J. (1992). Characterisation of three shoot apical meristem mutants of *Arabidopsis thaliana*. *Development*, 116, 397-403.

Ma, J., Lu, Y., Zhou, W., Zhu, Y., Dong, A., & Shen, W-H. (2018). Histone chaperones play crucial roles in maintenance of stem cell niche during plant root development. *Plant Journal,* 95, 86-100.

Machinandiarena, M.F., Oyarburo, N.S., Daleo, G.R., Andreu, A.B., & Olivieri, F.P. (2018). The reinforcement of potato cell wall as part of the phosphite-induced tolerance to UV-B radiation. *Biologia Plantarum,* 62, 388-394.

Melaragno, J.E., Mehrotra, B., & Coleman, A.W. (1993). Relationship between endopolyploidy and cell size in epidermal tissue of Arabidopsis. *The Plant Cell,* 5, 1661–1668.

Mozgova, I., Mokros, P., & Fajkus, J. (2010). Dysfunction of chromatin assembly factor 1 induces shortening of telomeres and loss of 45S rDNA in Arabidopsis thaliana. *The Plant Cell,* 22, 2768-2780.

Mozgova, I., Wildhaber, T., Liu, Q., Abou-Mansour, E., L'Haridon, F., Metraux, J.P., Gruissem, W., Hofius, D., & Hennig L. (2015). Chromatin assembly factor CAF-1 represses priming of plant defence response genes. *Nature Plants*, 1, 15127.

Muchova, V., Amiard, S., Mozgova, I., Dvorackova, M., Gallego, M.E., White, C., & Fajkus, J. (2015). Homology-dependent repair is involved in 45S rDNA loss in plant CAF-1 mutants. *Plant Journal*, 81, 198-209.

Muñoz-Viana, R., Wildhaber, T., Trejo-Arellano, M.S., Mozgova, I., & Hennig, L. (2017). Arabidopsis Chromatin Assembly Factor 1 is required for occupancy and position of a subset of nucleosomes. *Plant Journal*, 92, 363-374.

Ono, T., Kaya, H., Takeda, S., Abe, M., Ogawa, Y., Kato, M., Kakutani, T., Mittelsten Scheid, O., Araki, T., & Shibahara, K. (2006). Chromatin assembly factor 1 ensures the stable maintenance of silent chromatin states in Arabidopsis. *Genes Cells,* 11, 153-162.

Otero, S., Desvoyes, B., Peiro, R., & Gutierrez, C. (2016). Histone H3 Dynamics Reveal Domains with Distinct Proliferation Potential in the Arabidopsis Root. *The Plant Cell*, 28, 1361-1371.

Park, Y.J., & Luger, K. (2008). Histone chaperones in nucleosome eviction and histone exchange. *Current Opinion in Structural Biology*, 18, 282–289.

Pfluger, J., & Wagner, D. (2007). Histone modifications and dynamic regulation of genome accessibility in plants. *Current Opinion in Plant Biology*, 10, 645–652.

Pholo, M., Coetzee, B., Maree, H.J., Young, P.R., Lloyd, J.R., Kossmann, J., & Hills, P.N. (2018). Cell division and turgor mediate enhanced plant growth in *Arabidopsis* plants treated with the bacterial signalling molecule lumichrome. *Planta*, 248, 477-488.

Pontin, M.A., Piccoli, P.N., Francisco, R., Bottini, R., Martinez-Zapater, J.M., & Lijavetzky, D. (2010). Transcriptome changes in grapevine (Vitis vinifera L.) cv. Malbec leaves induced by ultraviolet-B radiation. *BMC Plant Biology*, 10, 224.

Radziejwoski, A., Vlieghe, K., Lammens, T., Berckmans, B., Maes, S., Jansen, M.A.K., Knappe, C., Albert, A., Seidlitz, H.K., Bahnweg, G., Inze´, D., & De Veylder, L. (2011). Atypical E2F activity coordinates PHR1 photolyase gene transcription with endoreduplication onset. *The EMBO Journal*, 30, 355–363.

Ramirez-Parra, E., & Gutierrez, C. (2007). E2F regulates FASCIATA1, a chromatin assembly gene whose loss switches on the endocycle and activates gene expression by changing the epigenetic status. *Plant Physiology*, 144, 105–120.

Rose, J.K.C., Braam, J., Fry, S.C., & Nishitani, K. (2002). The XTH family of enzymes involved in xyloglucan endotransglucosylation and endohydrolysis: current perspectives and a new unifying nomenclature. *Plant and Cell Physiology*, 43, 1421-1435.

Rosen, S., & Skaletsky, H.J. (2000). Primer3 on the WWW for general users and for biologist programmers. In Bioinformatics Methods and Protocols: Methods in Molecular Biology. Edited by Krawetz, S.A. and Misener S. pp. 365-386. Totowa NJ: Humana Press.

Ruiz, V.E., Interdonato, R., Cerioni, L., Albornoz, P., Ramallo, J., Prado, F.E., Hilal, M., & Rapisarda, V.A. (2016). Short-term UV-B exposure induces metabolic and anatomical changes in peel of harvested. *Journal of Photochemistry and Photobiology B: Biology*, 159, 59-65.

Sasidharan, R., Voesenek, L.A., & Pierik, R. (2011). Cell wall modifying proteins mediate plant acclimatization to biotic and abiotic stresses. *Critical Reviews in Plant Sciences*, 30, 548-562.

Schönrock, N., Exner, V., Probst, A., Gruissem, W., & Hennig, L. (2006). Functional genomic analysis of CAF-1 mutants in Arabidopsis thaliana. *Journal of Biological Chemistry*, 281, 9560-9568.

Stroud, H., Greenberg, M.V., Feng, S., Bernatavichute, Y.V., & Jacobsen, S.E. (2013). Comprehensive Analysis of Silencing Mutants Reveals Complex Regulation of the Arabidopsis Methylome. *Cell*, 152, 352-364.

Sugimoto-Shirasu, K., & Roberts, K. (2003). "Big it up": endoreduplication and cell-size control in plants. *Current Opinion in Plant Biology*, 6, 544–553.

Ulm, R., Baumann, A., Oravecz, A., Máté, Z., Adám, E., Oakeley, E.J., Schäfer, E., & Nagy F. (2004). Genome-wide analysis of gene expression reveals function of the bZIP transcription factor HY5 in the UV-B response of Arabidopsis. *Proceedings of the National Academy of Sciences USA*, 101, 1397–1402.

Vaillant, I., & Paszkowski, J. (2007). Role of histone and DNA methylation in gene regulation. *Current Opinion in Plant Biology*, 10, 528–533.

Varas, J., Sanchez-Moran, E., Copenhaver, G.P., Santos, J.L., & Pradillo, M. (2015). Analysis of the relationships between DNA double-strand breaks, synaptonemal complex and crossovers using the Atfas1-4 mutant. *PLoS Genetics*, 11, e1005301.

Verbsky, M.L., & Richards, E.J. (2001). Chromatin remodeling in plants. *Current Opinion in Plant Biology*, 4, 494–500.

Wargent, J.J., Gegas, V.C., Jenkins, G.I., Doonan, J.H., & Paul, N.D. (2009a). UVR8 in Arabidopsis thaliana regulates multiple aspects of cellular differentiation during leaf development in response to ultraviolet B radiation. *New Phytologist*, 183, 315–326.

Wargent, J.J., Moore, J.P., Roland Ennos, A., & Paul, N.D. (2009b). Ultraviolet radiation as a limiting factor in leaf expansion and development. *Photochemistry and Photobiology*, 85, 279–286.

Yan, A., Pan, J., An, L., Gan, Y., & Feng, H. (2012). The responses of trichome mutants to enhanced ultraviolet-B radiation in *Arabidopsis thaliana*. *Journal of Photochemistry and Photobiology B Biology,* 113, 29–35.

Yoshiyama, K.O., Kobayashi, J., Ogita, N., Ueda, M., Kimura, S., Maki, H., & Umeda, M. (2013). ATM-mediated phosphorylation of SOG1 is essential for the DNA damage response in *Arabidopsis*. *EMBO Reports,* 14, 817–822.

Zhang, X-Q., Wei, P-C., Xiong, Y-M., Yang, Y., Chen, J., & Wang, X-C. (2011). Overexpression of the Arabidopsis a-expansin gene AtEXPA1 accelerates stomatal opening by decreasing the volumetric elastic modulus. *Plant Cell Reports,* 30, 27–36.

Zhu, Y., Dong, A., & Shen, W-H. (2012). Histone variants and chromatin assembly in plant abiotic stress responses. *Biochimica et Biophysica Acta,* 1819, 343-348.

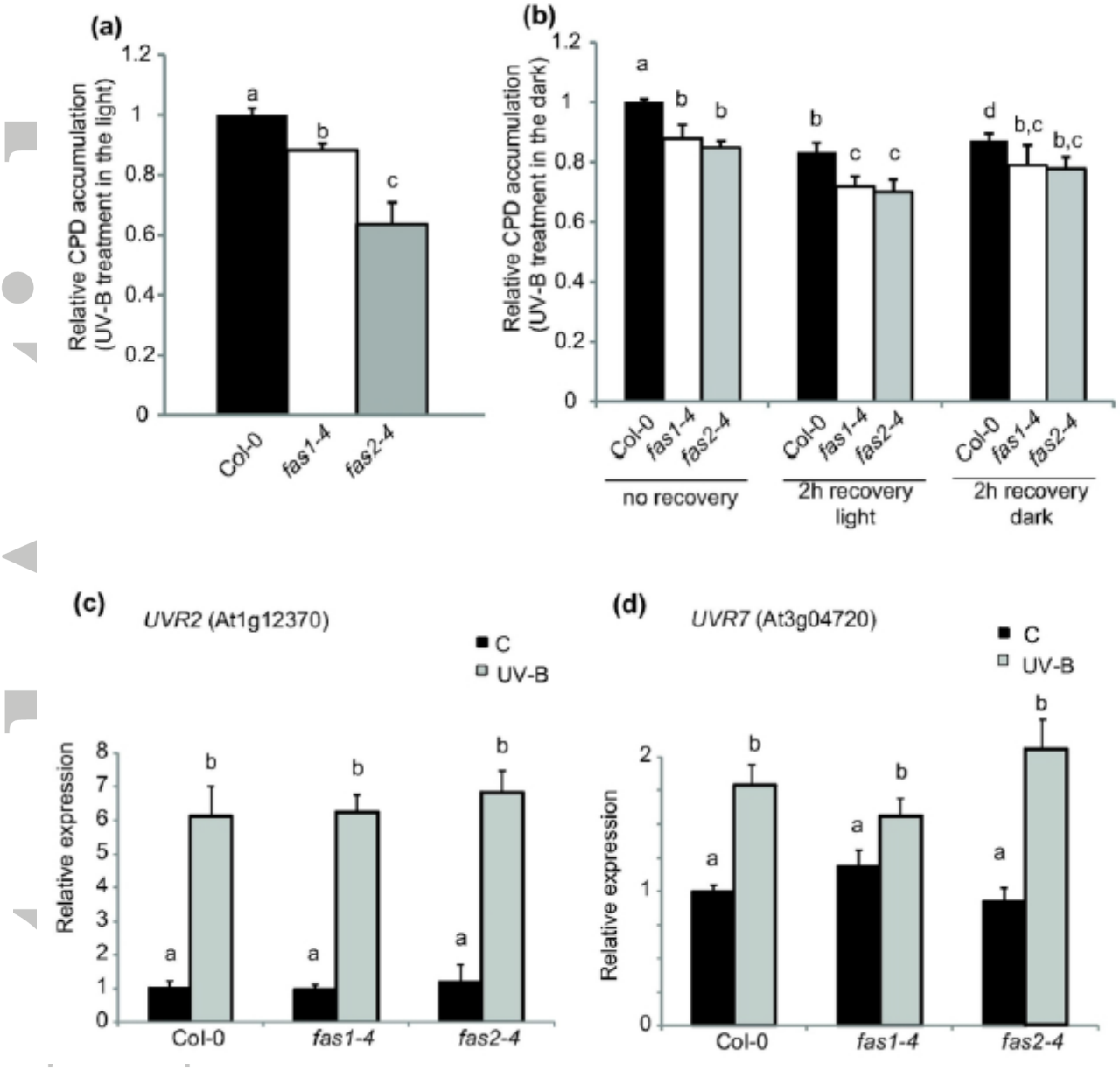

Figure 1 CPD levels in the DNA of WT, *fas1* and *fas2* mutant seedlings after UV-B exposure. (a) Relative CPD levels in the DNA of WT, *fas1-4* and *fas2-4* mutants immediately after a 4h-UV-B treatment under light conditions to allow photorepair to those in WT seedlings. (b) Relative CPD levels in the DNA of WT, *fas1-4* and *fas2-4* mutants immediately after a 4h-UV-B treatment under dark conditions, and 2h after recovery in the dark or under light conditions to allow photorepair to those in WT seedlings immediately after the 4h-UV-B treatment in the dark. (c,d) Relative expression levels of *UVR2* (c) and *UVR7* (d) determined by RT-qPCR analysis in Col-0, *fas1-4* and

fas2-4 leaf #5 under control conditions in the absence of UV-B (C), or immediately after a 4 h-UV-B treatment at 2 W m-2 (UV-B). Results represent the average ± S.D. of six independent biological replicates. Different letters denote statistical differences applying ANOVA test ($P < 0.05$).

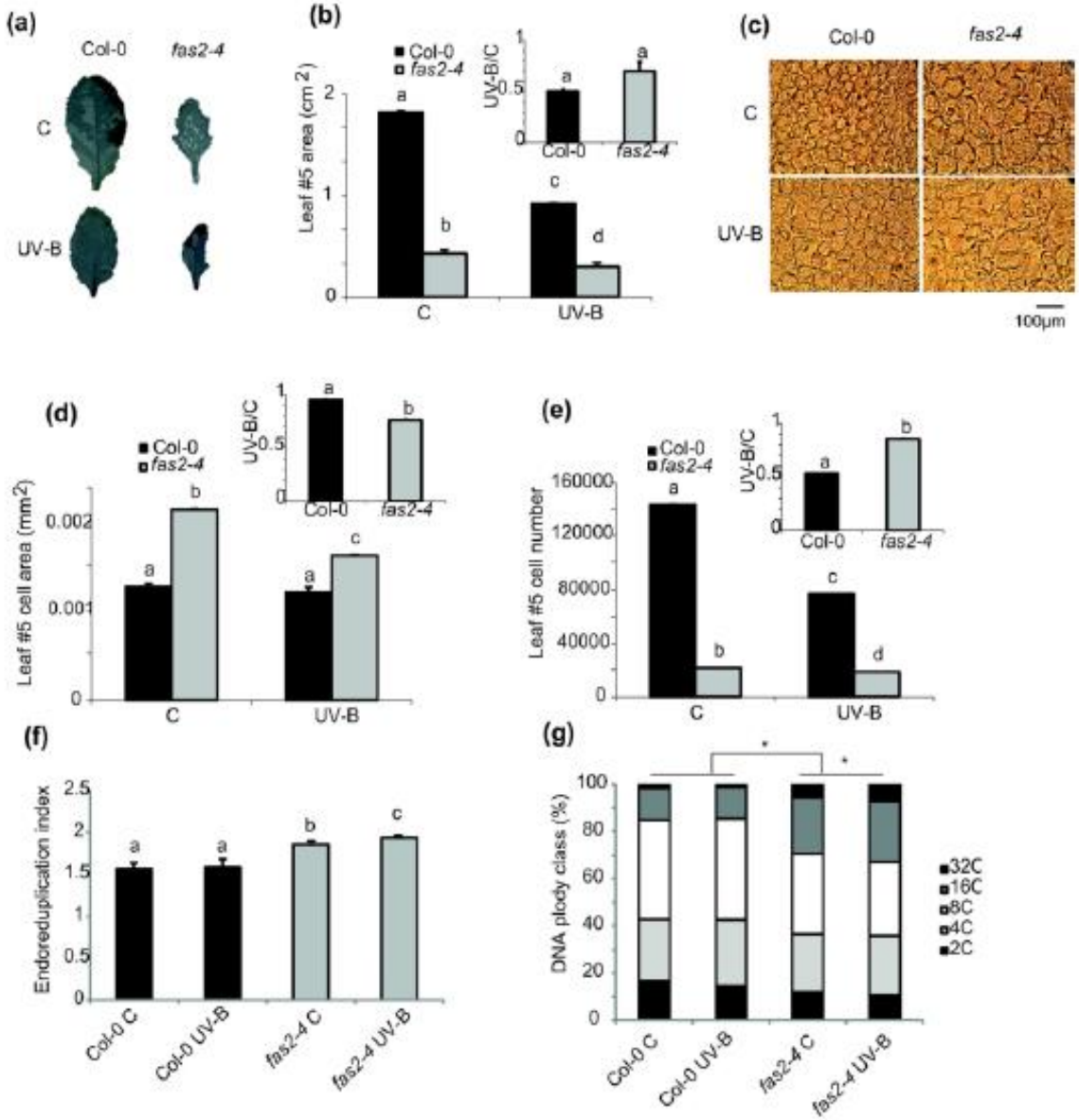

Figure 2 UV-B affects cell proliferation, cell expansion and DNA ploidy in proliferating leaves of CAF-1 mutants. (a) Silhouettes of fully expanded leaf #5 from UV-B treated or control Col-0 and *fas2-4* plants. (b) Average leaf area, (d) cell area and (e) cell number of fully expanded leaf #5 from UV-B treated or control Col-0 and *fas2-4* plants. Ratio between values measured after UV-B exposure relative to those under control conditions are shown as insets. (c) Images of leaf #5 cells from UV-B treated or control Col-0 and *fas2-4* plants. (f) Endoreduplication index of cells in leaf #5 from UV-B treated and control Col-0 and *fas2-4* plants. (g) Comparison of the nuclear DNA content

of Col-0 and *fas2-4* leaf #5 from UV-B treated and control Arabidopsis plants determined by flow cytometry. Results represent the average ± S.D. Different letters or an asterisk indicate statistical significant differences applying ANOVA test ($P < 0.05$).

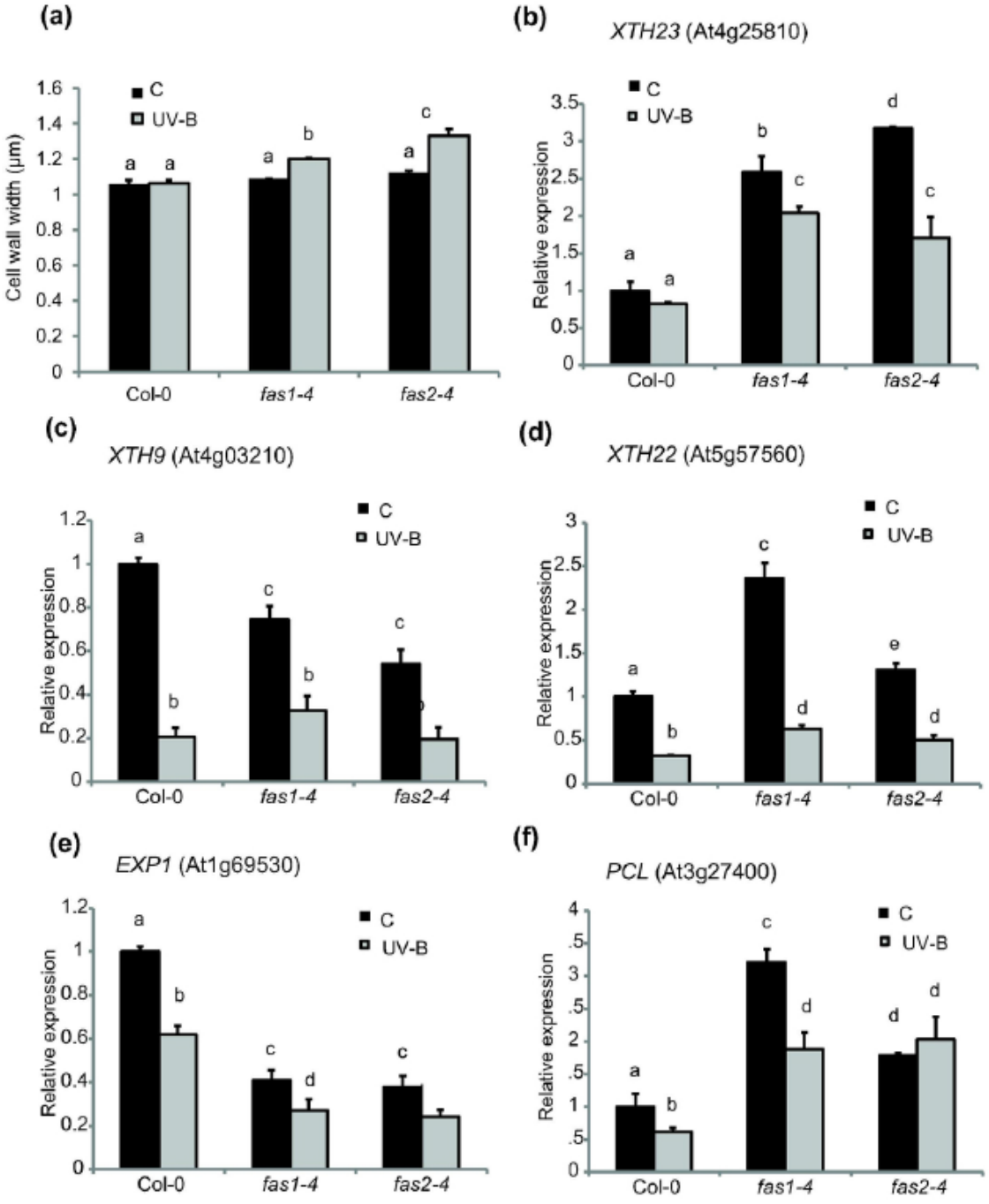

Figure 3 UV-B effect on leaf#5 cell wall and expression levels of cell wall metabolism enzymes in Col-0, *fas1* and *fas*2 plants. (a) Cell wall thickness in fully expanded leaf #5 from UV-B treated one week after the treatment or control Col-0, *fas1-4* and *fas2-4* plants. Graph of average cell wall width in leaf #5. (b-f) Relative expression levels of *XTH23* (b), *XTH9* (c), *XTH22* (d), *EXP1* (e) and *PCL* (f), determined by RT-qPCR analysis in Col-0, *fas1-4* and *fas 2-4* leaf #5 under control conditions in

the absence of UV-B (C), or one week after a 4 h-UV-B treatment at 2 W m^{-2} (UV-B). Results represent the average ± S.D. Different letters indicate statistical significant differences applying ANOVA test ($P < 0.05$).

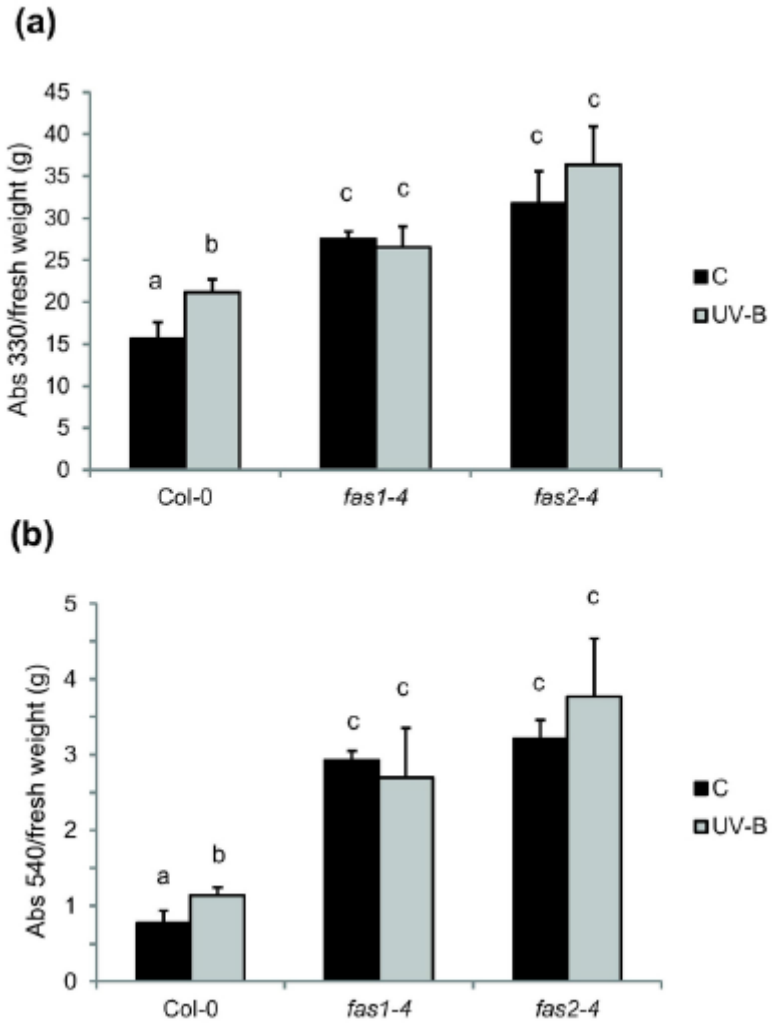

Figure 4 UV-B absorbing pigment content in Col-0 and CAF-1 mutants in leaves after UV-B exposure. (a,b) UV-B absorbing pigments (a) and anthocyanins (b) in Col-0, *fas1-4* and *fas2-4* leaves under control conditions (C), or after a 4 h-UV-B treatment (UV-B). Data represent 3 biological replicate experiments. Each experiment was repeated at least three times on each biological replicate.

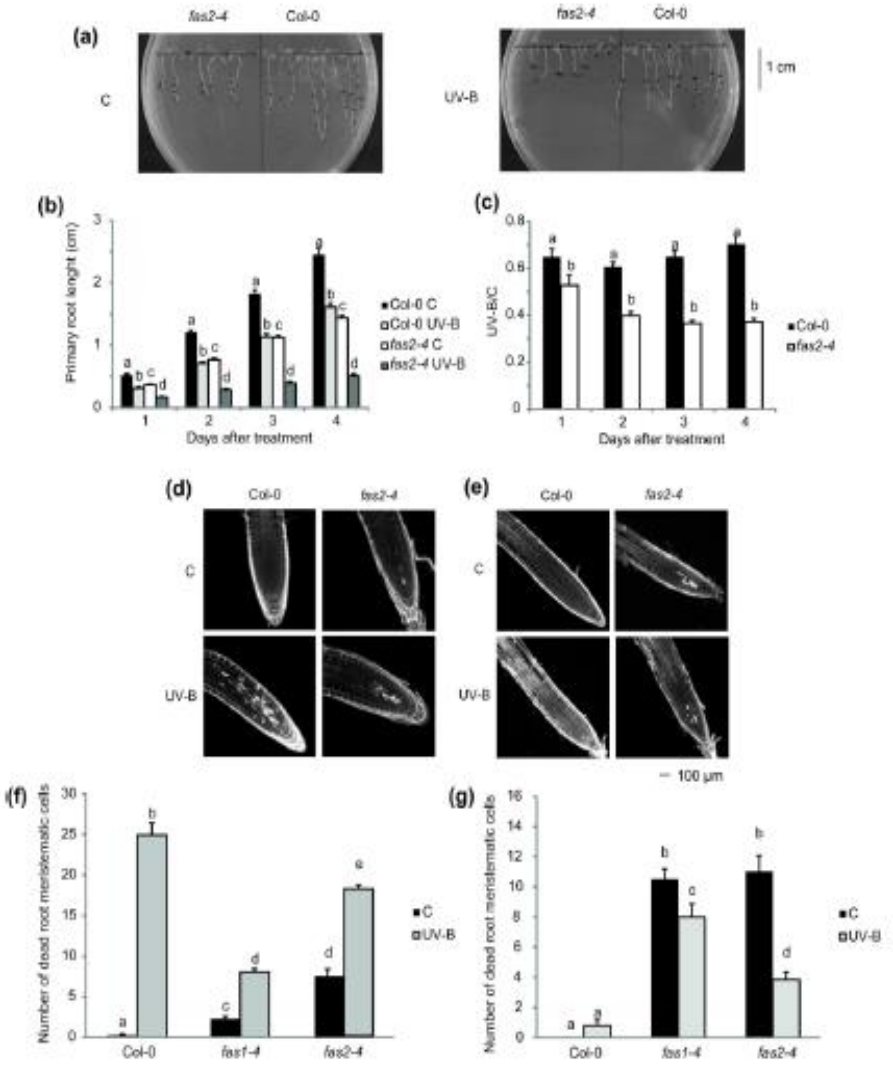

Figure 5 Primary root inhibition and programmed cell death in meristematic root cells in Col-0 and CAF-1 mutant plants after UV-B exposure. (a) Representative pictures of one experiment showing primary root inhibition assays in Col-0 and *fas2-4* seedlings after UV-B exposure or under control conditions. (b) Graph of average primary root length in Col-0 and *fas2-4* seedlings after UV-B exposure or under control conditions. (c) Ratio between values measured after UV-B exposure vs those under control conditions for Col-0 and *fas2-4* seedlings. Results represent the average of 30 biological replicates ± S.D. (d,e) Representative images of stem cells and adjacent daughter cells from WT Col-0 and *fas2-4* seedlings that were scored for intense PI staining to count dead stem cells per root 1d (d) and 4d (e) after a UV-B treatment or under control conditions. (f,g) Number of stem

cells that are dead under control conditions, after 1d (f) or 4d (g) of UV-B exposure in Col-0, *fas1-4* and *fas2-4* roots. Results represent the average of 10 biological replicates ± S.D. Different letters indicate statistical significant differences applying ANOVA test ($P < 0.05$).

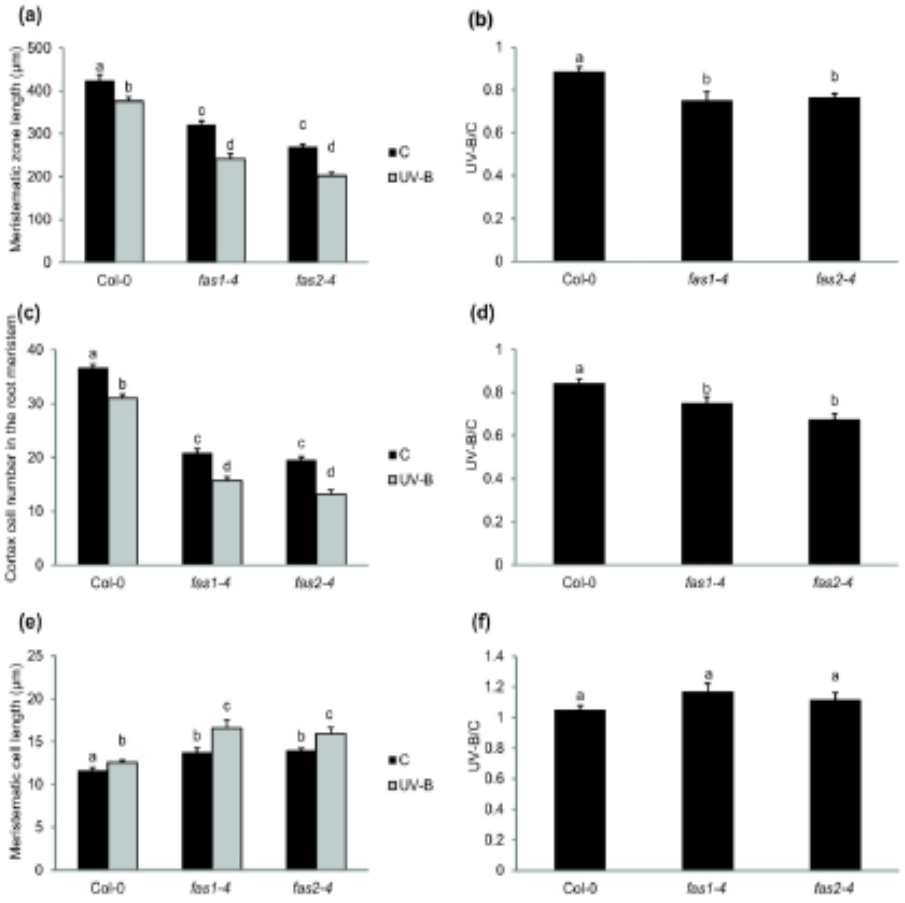

Figure 6 UV-B only affects cell proliferation in the root meristematic zone of *fas1* and *fas2* seedlings. (a) Average of meristematic root zone length, (c) cortex cell number and (e) cortex cell length in the root meristem from UV-B treated or control Col-0, *fas1-4* and *fas2-4* seedlings. (b, d and f) Ratio between meristematic root zone length (b), cortex cell number (d) and cortex cell area (f) values measured after UV-B exposure vs those under control conditions are shown. Results represent the average ± S.D. Different letters indicate statistical significant differences applying ANOVA test ($P < 0.05$).

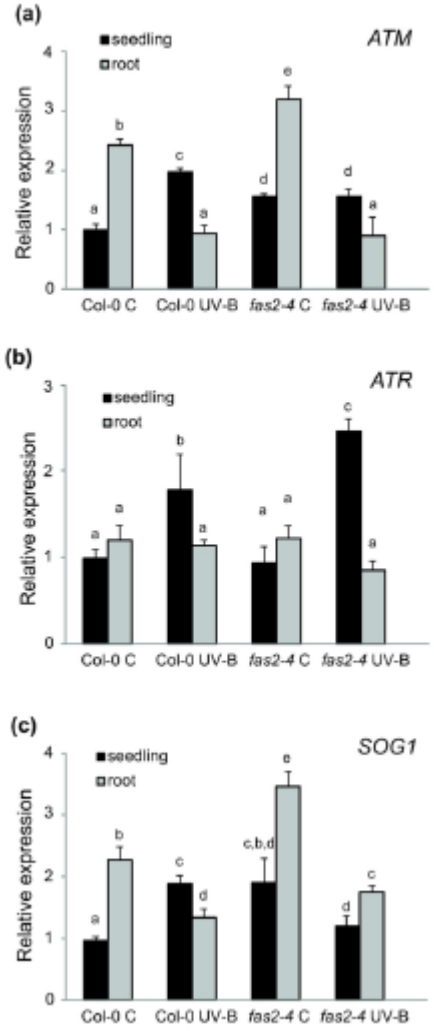

Figure 7 Expression of DNA damage response genes in Col-0 and CAF-1 seedlings and roots after UV-B. (a-c) UV-B effect on expression levels of *ATM* (a), *ATR* (b) and *SOG1* (c) in Col-0 and *fas2-4* seedlings and roots. Relative expression levels were determined by RT-qPCR under control conditions (C), or after a 4 h-UV-B treatment (UV-B). Results represent the average ± S.D. Different letters indicate statistical significant differences applying ANOVA test ($P < 0.05$). Data represent 3 biological replicate experiments. Each qRT-PCR was repeated at least three times on each biological replicate.